energies

Article

A Comparison of the Exergy Efficiencies of Various Heat-Integrated Distillation Columns

Areej Javed [1], Afaq Hassan [2], Muhammad Babar [2,*], Umair Azhar [2,*], Asim Riaz [2], Rana Mujahid [2], Tausif Ahmad [2], Muhammad Mubashir [3], Hooi Ren Lim [4], Pau Loke Show [4,5,6,*] and Kuan Shiong Khoo [7,*]

[1] School of Chemical Engineering, University of Engineering and Technology, Lahore 540000, Pakistan
[2] Chemical Engineering Department, Khwaja Fareed University of Engineering and Information Technology, Rahimyar Khan 64200, Pakistan
[3] Department of Petroleum Engineering, School of Engineering, Asia Pacific University of Technology and Innovation, Kuala Lumpur 57000, Malaysia
[4] Department of Chemical and Environmental Engineering, Faculty Science and Engineering, University of Nottingham Malaysia, Semenyih 43500, Malaysia
[5] Zhejiang Provincial Key Laboratory for Subtropical Water Environment and Marine Biological Resources Protection, Wenzhou University, Wenzhou 325035, China
[6] Department of Sustainable Engineering, Saveetha School of Engineering, SIMATS, Chennai 602105, India
[7] Department of Chemical Engineering and Materials Science, Yuan Ze University, Taoyuan 32003, Taiwan
* Correspondence: m.babar@kfueit.edu.pk (M.B.); dr.umairazhar@kfueit.edu.pk (U.A.); showpauloke@gmail.com (P.L.S.); kuanshiong.khoo@hotmail.com (K.S.K.)

Citation: Javed, A.; Hassan, A.; Babar, M.; Azhar, U.; Riaz, A.; Mujahid, R.; Ahmad, T.; Mubashir, M.; Lim, H.R.; Show, P.L.; et al. A Comparison of the Exergy Efficiencies of Various Heat-Integrated Distillation Columns. *Energies* **2022**, *15*, 6498. https://doi.org/10.3390/en15186498

Academic Editor: Iqbal M. Mujtaba

Received: 9 August 2022
Accepted: 29 August 2022
Published: 6 September 2022

Abstract: Distillation has relatively low thermodynamic efficiency, so it is a prime target for process intensification studies. The current research aims to study exergy losses in various heat-integrated distillation columns. A conventional industrial-scale i-butane/n-butane fractionator has been selected as a case study for the comparison of the performances of various heat-integrated designs. The Aspen Plus® process simulator is used to perform steady-state simulations and exergy analyses of the conventional distillation column (CDC), internally heat-integrated distillation column (iHIDiC), externally heat-integrated double distillation columns (EHIDDiC), and vapor recompression (VRC) systems. The results of these exergy analyses show that a modified VRC system (η_E = 10.69%) is the most efficient design for this separation. The exergy efficiency of the conventional VRC system is the same as that of the CDC (η_E = 9.27%). The EHIDDiC system (η_E = 9.77%) is somewhat better than the CDC, whereas iHIDiC shows poor exergy efficiency (η_E = 8.09%), even lower than the CDC.

Keywords: exergy; heat integrated distillation column; simulation

1. Introduction

In the chemical and petrochemical industries, distillation is the primary method of fluid separation and purification. However, the relatively low thermodynamic efficiency (5–20%) [1,2] of conventional distillation columns (CDC) makes them highly energy-intensive. Distillation accounts for 40–50% of the total plant operating cost in most refining and chemical processes [3]. A small improvement in the thermodynamic efficiency of distillation columns can, therefore, make a large difference in the overall process efficiency and profitability.

The exergy, or availability, of a system is defined as the maximum amount of work that can be extracted from it in a particular state and environment while still maintaining chemical, mechanical, and thermal equilibrium with that state and environment [4]. In other words, the exergy of a system is a measure of the disequilibrium between its current state and the environment. If a system is in complete thermodynamic equilibrium with its surroundings, it is said to have entered a "dead state". Dead state temperature and pressure are used as reference conditions for exergy analysis [5]. The exergy is conceptually different from Gibbs free energy, which requires the process to be isothermal and isobaric and, hence, involves no interaction with the environment [5].

Physical, chemical, kinetic, and potential exergy all contribute to a system's total exergy. In most cases, the exergy terms associated with kinetic and potential energy are negligible [6]. In order to get from the system's current state (T, P) to the ideal state (T0, P0), the maximum amount of useful work that can be extracted from the system is called the physical exergy. To compensate for the discrepancy between the system's actual composition and the environment's composition, the chemical exergy is the maximum amount of useful work achieved in achieving chemical equilibrium.

Irreversibilities in a process, as stated by the second law of thermodynamics, result in an overall increase in entropy and a decrease in energy quality. In this way, exergy analysis [7] evaluates the energy efficiency of the process and allows for the identification of the sources of irreversibility by providing a measure of both the quantity and quality of energy available in the process [8]. An increase in available energy results from a decrease in exergy destruction, which in turn increases the efficiency of the process as a whole.

Exergy losses in a distillation column are due to the difference between the exergy entering the column and the exergy leaving the column. In a CDC, heat is supplied only through the main reboiler and rejected only through the main condenser, while the column operates adiabatically. Exergy input to a CDC includes exergy of the feed stream plus exergy input to the main reboiler. Similarly, the exergy output of a CDC includes the exergy of the product streams plus exergy leaving the main condenser. Exergy losses in a CDC are, therefore, directly associated with the condenser and reboiler duties. In fact, the temperature difference between the reboiler and the condenser is the main reason for the considerable degradation of thermal energy and the energy inefficiency of the conventional distillation technique.

There have been a great deal of complex modifications to and departures from traditional distillation processes as a result of the search for improved methods [9]. Among non-conventional distillation technologies, heat-integrated distillation processes [2] have received particular attention due to potentially substantial energy savings. An important feature of such heat-integrated distillation processes is a net reduction in utility costs, which often results in higher energy efficiency.

Distillation columns typically have a diabatic section that allows for heat transfer between the stages. Therefore, the main utility load and the overall exergy loss of the section are reduced as the exergy losses from the main condenser or main reboiler are distributed to other stages of the respective section [10]. Two diabatic sections with counterclockwise heat transfer are combined in an internally heat-integrated distillation column (iHIDiC) [11]. The total heat rejected is, thus, distributed along the rectification section, and the total heat absorbed is likewise distributed along the stripping section. The temperature driving force required for heat transfer between the two sections is the pressure difference between the two sections, which is controlled by a compressor and a throttling valve. Since there isn't much of a temperature swing between the two stages in a heat integration process, the exergy losses associated with heat transfer are reduced, resulting in a lower net energy demand for both stages [10].

Direct vapor recompression and heat integration between diabatic sections characterize an iHIDiC. There can be heat integration at any stage along the column sections, moving heat from the rectifying section to the stripping section. Furthermore, it is not required that the number of stages in the rectifying and stripping sections be the same [12]. Modifying the compression ratio generates the temperature driving force required for heat transfer between the two sections. This means that the rectifying section is subjected to significantly greater pressure than the stripping section while in operation. The iHIDiC can be thought of as a self-heat recovery system due to the fact that it uses heat-integrated stages to perform the functions of both condensers and reboilers. The primary condenser and reboiler will require less direct utility thanks to this setup.

The stripping section of an iHIDiC typically has a higher vapor flow than the rest of the device because of the progressive evaporation of the descending liquid on heat-integrated stages. However, the total vapor flow in the rectifying section is diminished as the condensation of ascending vapor occurs. IHIDiC typically have a vapor flow area that can be adjusted along its length to account for the wide range of vapor flows that may be encountered.

To realize heat integration in iHIDiC systems, various heat transfer arrangements have been proposed. These include Super HIDiC, shell-and-tube exchanger columns, plate-fin exchanger columns, concentric columns, inter-coupled distillation columns, and concentric columns with partition walls [13–18]. Furthermore, a uniform heat transfer area approach or uniform heat distribution approach can be used to distribute heat integration [10,19].

The liquid feed is split between two distillation columns operating at different pressures and an integrated condenser-reboiler setup in an externally heat-integrated double distillation column (EHIDDiC) [20]. It is possible to balance the workloads of the high-pressure (HP) column's condenser and the low-pressure (LP) column's reboiler by adjusting the feed split between the two columns. EHIDDiC systems are typically easier to design and operate than iHIDiC systems due to the fact that heat exchange occurs away from the column shells. When a pump is used in place of a compressor, energy consumption drops dramatically.

In essence, an EHIDDiC system is just a tweaked iHIDiC. The iHIDiC is a distillation column with heat integration set up between the rectifying and stripping sections. Heat integration, on the other hand, is set up in an EHIDDiC system between the rectifying section of one distillation column and the stripping section of another [21]. By doing so, we can run the two columns at different pressures and switch from a costly vapor compression process to a much more cost-effective liquid pumping operation.

Heat transfer requires a temperature driving force, which can be generated by controlling the column pressure. By adjusting the feed split, "neat mode" ensures that the HP column's condenser duty and the LP column's reboiler duty are balanced. Through this set-up, we are able to combine the two processes and get rid of one heat exchanger. External heat exchangers placed in strategic locations can also be used to integrate heat between the heat-integrated sections [21]. Symmetrical EHIDDiC is characterized by an equal number of stages in both the rectifying section of the HP column and the stripping section of the LP column [21]. The asymmetrical EHIDDiC configuration is more adaptable because the heat-integrated sections have different numbers of stages.

The energy of the vapor above is combined with mechanical energy from a compressor in a vapor recompression (VRC) system [22] to boil the liquid below. The pressure ratio needed to raise the overhead vapor temperature to a point where heat transfer from compressed overhead vapor to the bottom product is feasible has a significant impact on the compressor duty. Systems that require only a modest boost in the energy quality of the overhead vapor (i.e., close-boiling systems) can benefit most from VRC designs [23]. Furthermore, a VRC system is generally the most practical method of implementing heat integration in an already existing distillation system through revamping, as it only requires a single conventional column shell.

Vapor recompression (VRC) systems work by compressing the vapor at the top to raise its temperature above the liquid at the bottom. Using a condenser and a reboiler in tandem, the superheated vapor is condensed and then used to boil the bottoms liquid. Liquid reflux is provided by the condensate, which is restricted to a pressure just below the column's top. Vaporization of the bottom liquid provides the required vapor boil-up [22]. For the separation of close-boiling mixtures, where the temperature differential between the condenser and the reboiler is small, and where small compression ratios are sufficient to heat the overhead vapor and create the necessary temperature driving force for heat transfer, VRC systems are ideally suited.

The separation of a methanol/water mixture was proposed by Shahandeh et al. [24], who also suggested five heat pump-assisted schemes. While there is little economic benefit in separating the wide-boiling mixtures, VRC's high energy efficiency necessitates a small temperature difference between the top and bottom of the distillation column [25,26]. For the purpose of purifying ethyl acetate and ethanol, Zhu et al. [27] investigated the use of ionic liquids (ILs) as solvents for extractive distillation and obtained the design parameters of an extractive distillation process with a solvent recovery system. A mixture of 50% ethanol and 50% tetrahydrofuran was separated using extractive distillation (ED) and partially heat-integrated pressure-swing distillation (PHIPSD) using dynamic controls [28]. Separating benzene, isopropanol, and water ternary mixtures via dividing-wall column distillation was studied by Li et al. [29]. The total annual cost (TAC) decreased by 28.6 percent, and carbon dioxide emissions decreased by 32.8 percent. Separating acetonitrile, benzene, and methanol, Wang et al. [30] compared a novel thermally coupled extractive distillation sequence. This study found that side-stream extractive distillation significantly reduced TAC and CO_2 emissions (by 32.84 and 38.41 percent, respectively) and had a positive impact on the economy and the environment. However, the DWC will not result in a systemwide economic benefit. In their study, Brito et al. [31] looked into the feasibility of separating mixtures of ethanol/water, tetrahydrofuran/water, and acetone/methanol. The results demonstrated that the separation was not always best using the thermally coupled extractive distillation sequence. The novel heat-pump-assisted extractive distillation studied by Luo et al. [32] has been found to be 40% more energy efficient and 24% less toxic than DWC. Qi et al. [33] investigated the use of azeotropic and extractive distillation with heat integration to separate the heterogeneous ternary azeotropes, diisopropyl ether, isopropyl alcohol, and water. Results showed that the heat integration schemes saved 29.78% and 42.19% of energy compared to traditional distillation. In order to reduce total energy consumption by 27% when compared to conventional extractive distillation, Gui et al. [34] proposed an improved heat integration extractive distillation with a recycle feed. To address the excessive energy requirements proposed by Cui et al. [35], Jian et al. [36] investigated five distinct configurations of extractive distillation (ED) to have the highest TAC, lowest energy consumption, lowest CO_2 emissions, highest exergy destruction, and highest exergy efficiency. Yan et al. [37] investigated the feasibility of developing side-stream hybrid reactive-extractive distillation (SS-DCRED) to recover isopropanol and ethyl acetate from wastewater. Total energy consumption, TAC, and environmental efficiency are the primary research foci. Thus, there is a need to study the exergy losses and thermodynamic efficiency of the different heat integrated columns.

In this work, a conventional industrial-scale i-butane/n-butane fractionator has been selected as a case study for the comparison of the performances of various heat-integrated designs. Because of the small relative volatility between the two key components, such columns require a large number of theoretical stages and must be operated at high reflux ratios, leading to large column diameters and increased condenser and reboiler duties. These attributes make such separations an excellent target for process intensification studies. The column under consideration is 51.8 m with a diameter of 2.9 m and contains 74 two-pass valve trays. It operates with a condenser pressure of 658.6 KPa and subcooled reflux at 18.5 °C. Complete column specifications and performance data are listed in Tables 1 and 2, respectively.

Table 1. Reconciled data of stream compositions and flows [38,39].

	Feed (Exp)	Feed (Simulated)	Distillate (Exp)	Distillate (Simulated)	Bottoms (Exp)	Bottom (Simulated)
Propane, wt. fraction	0.0154	0.0154	0.0494	0.0495	0.0000	0.0000
i-Butane, wt. fraction	0.2950	0.2949	0.9420	0.9419	0.0300	0.0029
n-Butane, wt. fraction	0.6770	0.6768	0.0020	0.0020	0.9810	0.9821
i-Butene, wt. fraction	0.0013	0.0013	0.0023	0.0033	0.0008	0.0004
1-Butene, wt. fraction	0.0020	0.0020	0.0041	0.0051	0.0010	0.0006
neo-Pentane, wt. fraction	0.0011	0.0011	0.0000	0.0000	0.0017	0.0016
i-Pentane, wt. fraction	0.0077	0.0077	0.0000	0.0000	0.0112	0.0112
n-Pentane, wt. fraction	0.0008	0.0008	0.0000	0.0000	0.0011	0.0012
Total flow, kg/h	26,122	26,122	8123	8123	17,999	17,999

This study focuses on the five different cases, all of which involve a comparison between Heat Integrated Columns and more traditional distillation methods. The comparison is based on thermodynamic efficiency. The i-butane/n-butane mixture is used in the case studies. Using an exergy analysis of the Aspen Plus simulations, this project aims to determine the optimal heat-integrated configuration.

2. Exergy Analysis

When applied to the design, optimization, and improvement of various thermodynamic systems, exergy analysis proves to be an invaluable tool. Recent research shows [40] that it is used in a wide variety of manufacturing settings, including paper factories, aluminum and iron foundries, chemical and petrochemical industries, and sugar and cement production. Energy efficiency improvements in these fields have been demonstrated to be a viable future goal. This enhancement can be backed by exergy analysis, which can reveal hidden losses. Modern lean management, as introduced by Haragovics and Mizsey [41], also supports this idea. Their research demonstrates how exergy analysis can be used to uncover the latent potentials of the lean philosophy, which highlights the inflexibility and hidden losses that render industrial chemical processes inefficient. Examining the system's thermodynamic efficiency, as exergy analysis does, allows for the prediction of economic study outcomes [42]. Being founded on the two fundamental laws of thermodynamics, the exergy analysis method has been around for quite some time [43]. Every energy system can be analyzed using an energy balance based on the first law. However, according to the second law, not all heat energy can be converted to useful work, so an exergy balance is more appropriate. Exergy demonstrates the magnitude and nature of energy by being the maximum amount of energy present in a system as it degenerates to a dead state [44,45].

The total exergy of a material stream E [kW] is a product of its molar exergy, and molar flow rate. When kinetic and potential exergy terms are neglected, the molar exergy of a material stream includes only physical and chemical exergies [46]

$$e = e^{ph} + e^{ch} \tag{1}$$

e^{ch}, the molar chemical exergies for the components are mentioned in Table 2. The molar physical exergy, e^{ph} [kJ/mol], of a material stream is calculated using its molar enthalpy and molar entropy relative to a reference environment [46].

$$e^{ph} = (h - h_0) - T_0(s - s_0) \tag{2}$$

where T_0 [K] is the reference temperature and P_0 [Pa] is the reference pressure. h [kJ/mol] and h_0 [kJ/mol] are molar enthalpies of the stream at actual conditions (T, P) and reference conditions (T_0, P_0), respectively. Similarly, s [kJ/(mol.K)] and s_0 [kJ/(mol.K)] are molar entropies of the stream at actual and reference conditions, respectively. In this work, T_0 = 298.15 K and P_0 = 101,325 Pa have been selected as reference conditions.

The values of molar enthalpy and molar entropy at actual conditions are obtained from the converged steady-state simulation model. The corresponding values at reference conditions are determined by changing the temperature and pressure of the stream to reference conditions using a duplicator block coupled with a simple heater/cooler model.

Table 2. Standard chemical exergies of gas-phase components at 298.15 K and 101,325 Pa [47,48].

Component	$e^{ch}(\frac{\mathbf{kJ}}{\mathbf{mol}})$
Propane	2154.00
i-Butane	2803.41
n-Butane	2805.80
i-Butene	2646.28
1-Butene	2659.70
neo-Pentane	3452.49
i-Pentane	3452.70
n-Pentane	3463.30

The total exergy of a thermal energy stream is calculated as

$$E_q[\mathrm{kW}] = \left(1 - \frac{T_0}{T}\right) \cdot Q[\mathrm{kW}] \tag{3}$$

where heat load, Q, is positive when heat is added to the system (i.e., reboiler duty) and negative when heat is removed from the system (i.e., condenser duty).

The total exergy of a mechanical work stream is equal to the net shaft work.

$$E_w[\mathrm{kW}] = W[\mathrm{kW}] \tag{4}$$

For a distillation column, the minimum amount of work, ΔE_{min} [kW], required for the separation is equal to the total exergy of product streams minus the total exergy of feed streams [28].

$$\Delta E_{min}[\mathrm{kW}] = \sum_{products} E_j - \sum_{feeds} E_i \tag{5}$$

On the other hand, the actual work, E_{act} [kW], consumed to achieve the same separation is the sum of exergies of utility loads [28].

$$E_{act}[\mathrm{kW}] = \sum_{utilities} E_k \tag{6}$$

Exergy efficiency of a distillation column, η_E, [28] is then calculated as

$$\eta_E[\%] = \frac{\Delta E_{min}}{E_{act}} \times 100 \tag{7}$$

3. Results and Discussion

3.1. Exergy Analysis of the Conventional Distillation Column

The simulation model of the CDC system has been adopted from the work of Kanwal [49]. In this model, the CDC system is simulated as an equilibrium-based RadFrac® column with the Soave–Redlich–Kwong (SRK) property package using Aspen Plus® (Version 9.0). Stage efficiencies are adjusted to reproduce the reported data of column duties and stage temperatures [38,39] and product compositions and flow rates (Table 1). Using the predicted stage efficiency of 137.9%, the number of theoretical stages in the conventional column is calculated to be 104. A new simulation model (Figure 1) is then developed containing 104 theoretical stages with 100% stage efficiency.

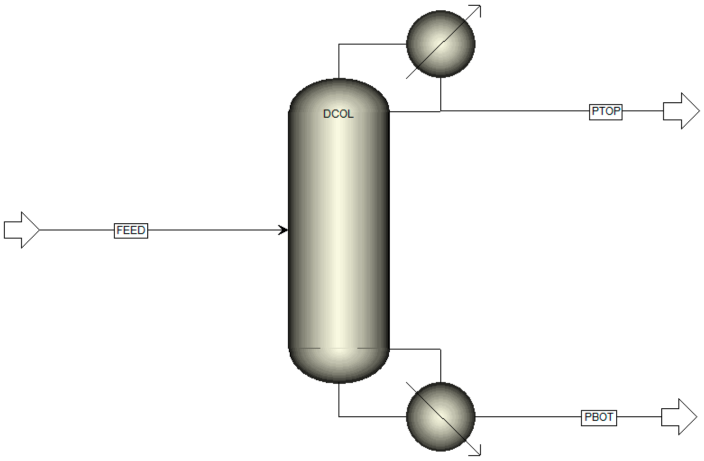

Figure 1. Schematic representation of the CDC model in Aspen Plus®.

Table 3 summarizes the results of the exergy analysis of the CDC system. As expected for a close-boiling mixture, the exergy efficiency of the CDC is very low (9.27%). This is due to the large reflux ratio required to achieve this separation, which results in large condenser and reboiler duties.

Table 3. Exergy analysis of the CDC system.

ID	*E*(kW)
FEED	350,324
PTOP	108,979
PBOT	241,510
QREB	1193
QCOND	−548
QSUBC	−39
Exergy minimum	165
Exergy actual	1779
Exergy efficiency (%)	9.27

3.2. Exergy Analysis of the Internally Heat-Integrated Distillation Column

The simulation model of the iHIDiC system has been adopted from the work of Kanwal [49]. In this model, the iHIDiC system is simulated using two equilibrium-based RadFrac® columns with the Soave–Redlich–Kwong (SRK) property package using Aspen Plus® (Version 9.0). Each column contains 76 theoretical stages. A compression ratio of 1.60 is maintained in the compressor. The columns are heat-integrated using a uniform heat transfer area approach with three side heat exchangers. For simplicity, these side heat exchangers are modelled as side heat streams to the two columns (Figure 2). To make a fair comparison with the CDC system, all products are brought to the same thermodynamic conditions as obtained in the reference CDC simulation.

Table 4 summarizes the results of the exergy analysis of the iHIDiC system. Surprisingly, the exergy efficiency of the iHIDiC system is very low (8.09%). In fact, it is even lower than the existing CDC system.

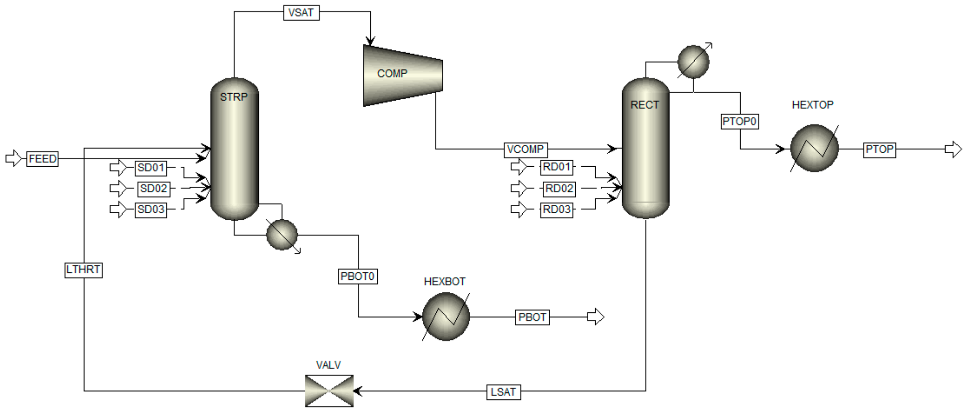

Figure 2. Schematic representation of the iHIDiC model in Aspen Plus® [49].

Table 4. Exergy analysis of the iHIDiC system.

Stream	*E*(kW)
FEED	350,324
PTOP	108,685
PBOT	241,822
QREB	466
QCOND	−461
QSUBC	−31
QHEXTOP	−7
QHEXBOT	21
VCOMP	1283
RD01	−311
RD02	−306
RD03	−578
SD01	247
SD02	253
SD03	435
Exergy min.	183
Exergy act.	2269
Exergy efficiency (%)	8.09

3.3. Exergy Analysis of the Externally Heat-Integrated Double Distillation Columns

The simulation model of the EHIDDiC system has been adopted from the work of Sadaf [50]. In this model, the EHIDDiC system is simulated using two equilibrium-based RadFrac® columns with the Soave–Redlich–Kwong (SRK) property package using Aspen Plus® (Version 9.0). The LP and the HP columns contain 119 and 173 theoretical stages, respectively. The LP column operates at the same conditions as the CDC, whereas the HP column operates at 2.5 times higher pressure to ensure a temperature driving force ≥ 20 °C between the condenser of the HP column and the reboiler of the LP column.

The feed is pumped to the pressure of the HP column before being split between the two columns as shown in Figure 3. The feed split ratio is manipulated to operate the system in "neat mode" such that the duties of the HP condenser and LP reboiler are equalized. The top and bottom product purities of both columns are constrained to match those obtained from the CDC system. In addition, to make a fair comparison with the CDC system, products from the HP column are brought to the same thermodynamic conditions as obtained in the reference CDC simulation.

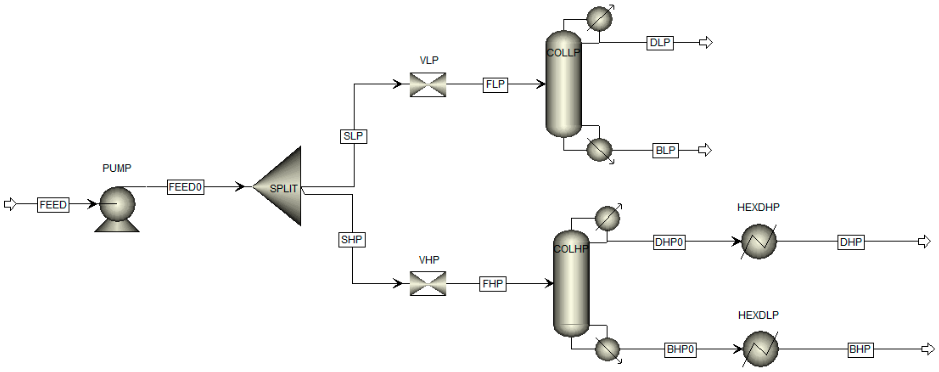

Figure 3. Schematic representation of the EHIDDiC model in Aspen Plus® [50].

Table 5 summarizes the results of the exergy analysis of the EHIDDiC system. The overall exergy efficiency of the EHIDDiC system (9.77%) is considerably better than that of the existing CDC system.

Table 5. Exergy analysis of the EHIDDiC system.

ID	*E*(kW)
FEED	350,324
DLP	44,805
DHP	63,961
BLP	99,551
BHP	142,181
QREBHP	1447
QCONDLP	203
QSUBCLP	14
QSUBCHP	59
QHEXDHP	10
QHEXBHP	32
WPUMP	19
QCONDHP	638
QREBLP	443
Exergy minimum	174
Exergy actual	1783
Exergy efficiency (%)	9.77

3.4. *Exergy Analysis of the Conventional Vapor Recompression System*

The simulation model of the conventional VRC system has been adopted from the work of Maria [51]. In this model, the VRC system is simulated using an equilibrium-based RadFrac® column with the Soave–Redlich–Kwong (SRK) property package using Aspen Plus® (Version 9.0). The column specifications are the same as the CDC system. The vapor stream leaving the top of the column is compressed and used to boil the liquid stream leaving the bottom of the column as shown in Figure 4. A compression ratio of 2.0 is maintained in the compressor to ensure a sufficient temperature driving force for heat transfer. A fraction of the partially vaporized liquid stream leaving the integrated heat exchanger is drawn as the bottom product, while the remainder is vaporized and fed to the column as vapor boil-up. The partially condensed vapor stream leaving the integrated heat exchanger is throttled and completely condensed. A fraction is drawn as the top product, while the remainder is subcooled and fed to the column as liquid reflux.

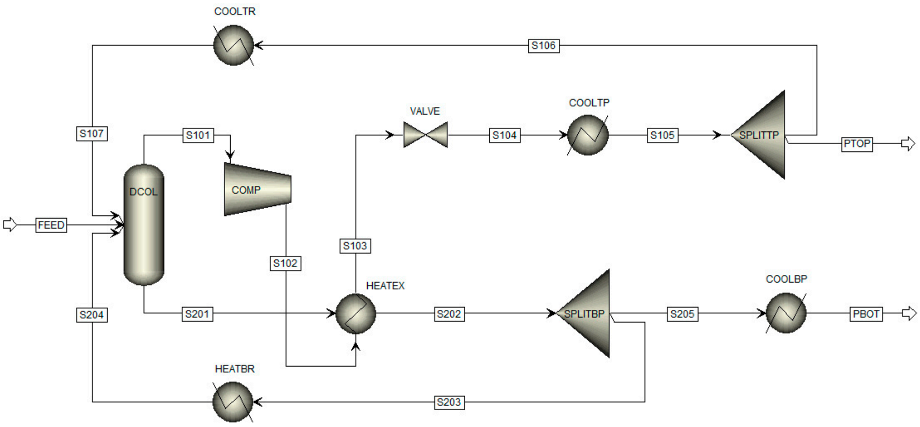

Figure 4. Schematic representation of the conventional VRC model in Aspen Plus® [51].

Table 6 summarizes the results of the exergy analysis of the conventional VRC system. The overall exergy efficiency of the conventional VRC system (9.27%) is the same as the existing CDC system. A closer look at the results reveals that heat integration considerably reduces thermal energy duties. In fact, this reduction in exchanger duties is even more pronounced than the iHIDiC system. However, the mechanical work of compression required to achieve this reduction in thermal energy duties is rather high, resulting in the cancellation of the gains in exergy efficiency.

Table 6. Exergy analysis of the conventional VRC system.

Stream	***E*(kW)**
FEED	350,324
PTOP	108,705
PBOT	241,782
QHEATBR	436
QCOOLTP	143
QCOOLTR	38
QCOOLBP	117
WCOMP	1031
HEXVAP	1089
HEXLIQ	851
Exergy min.	164
Exergy act.	1765
Exergy efficiency (%)	9.27

3.5. Exergy Analysis of the Modified Vapor Recompression System

A closer look at the conventional VRC system, as shown in Figure 5, reveals a poor heat transfer arrangement in the bottom loop. The whole liquid stream leaving the bottom of the column is boiled using compressed vapor, while only a fraction of it is to be sent back to the column. In other words, in the conventional VRC system, a fraction of the bottom liquid is first heated in the integrated heat exchanger, only to be cooled later as a bottom product. A simple rearrangement in the bottom loop can fix this issue.

Figure 5 shows a schematic representation of the modified VRC system. Since the liquid stream leaving the bottom of the column is already at the desired conditions, a fraction of it can be drawn as the bottom product. As in the modified VRC, a total reboiler is applied instead of the partial reboiler. The remaining fraction is first heated in the integrated heat exchanger using compressed vapor and then completely vaporized before being fed to the column as vapor boil-up. This arrangement not only eliminates one heat exchanger, but also further reduces the thermal energy duties.

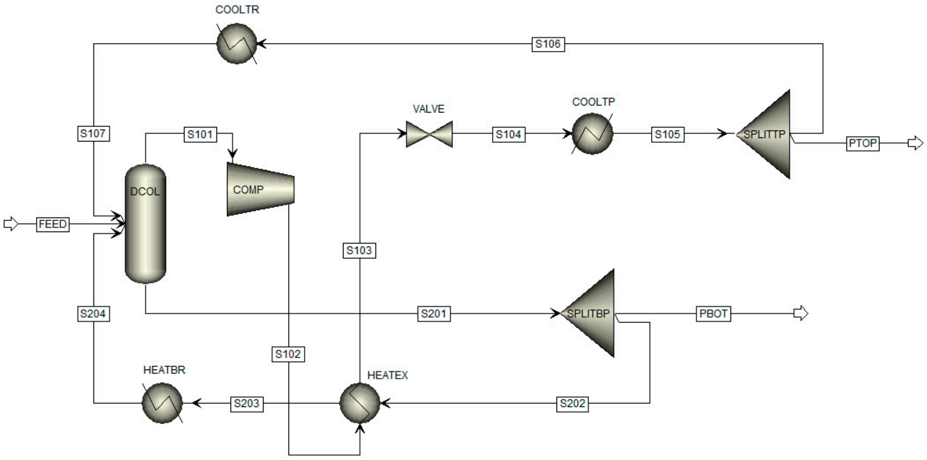

Figure 5. Schematic representation of the modified VRC model in Aspen Plus® [51].

Table 7 summarizes the results of the exergy analysis of the modified VRC system. As expected, pre-splitting the bottom liquid before the integrated heat exchanger reduces the reboiler duty by the same amount as previously required to cool the bottom product. All other thermal and mechanical utility requirements remain the same as observed in the conventional VRC system. As the total utility requirements decrease, the overall exergy efficiency of the system increases to 10.69%.

Table 7. Exergy analysis of the modified VRC system.

Stream	E(kW)
FEED	350,324
PTOP	108,705
PBOT	241,782
QHEATBR	319
QCOOLTP	143
QCOOLTR	38
WCOMP	1031
HEXVAP	1089
HEXLIQ	851
Exergy min.	164
Exergy act.	1531
Exergy efficiency (%)	10.69

Figure 6 shows the exergy flow diagrams for all of the configurations. The exergy distribution across all the sections in the configurations can be easily understood.

Table 8 summarizes the results of exergy analyses of alternative heat-integrated designs for the i-butane/n-butane fractionator. The selection of an appropriate heat integration scheme is critical for improving the overall exergy efficiency of the separation system. While all heat integration schemes explored in this project show an apparent reduction in total utility requirements, a proportional increase in overall exergy efficiency is not observed in all cases. It is, therefore, important to account for both the magnitude as well as the quality of energy required for a given separation. For example, expending 1 MW of mechanical energy in compression to achieve a 1 MW reduction in reboiler duty is impractical. Similarly, a 1 MW reduction in the duty of a water-cooled condenser at the expense of a 1 MW increase in the duty of a refrigerated condenser is impractical. Moreover, appropriate matching of hot and cold streams when implementing heat integration in a system is also critical. For example, a simple rearrangement of the bottom loop in the VRC system, not only eliminates one heat exchanger, but also improves the overall exergy efficiency of the system by over 15% relative to the conventional distillation column. Similarly, for the HIDiC, the heat integration indeed reduces both the condenser and the reboiler duties. However, the reduction in thermal energy duties is much smaller than the mechanical work of compression required to achieve this reduction. Since mechanical energy is a more refined form of energy as compared to thermal energy, the total utility requirements to achieve the same degree of separation are significantly higher, resulting in a lower overall exergy efficiency. However, the replacement of the compressor (iHIDiC system) with a pump (EHIDDiC system) considerably reduces the mechanical work requirements, leading to higher overall exergy efficiency.

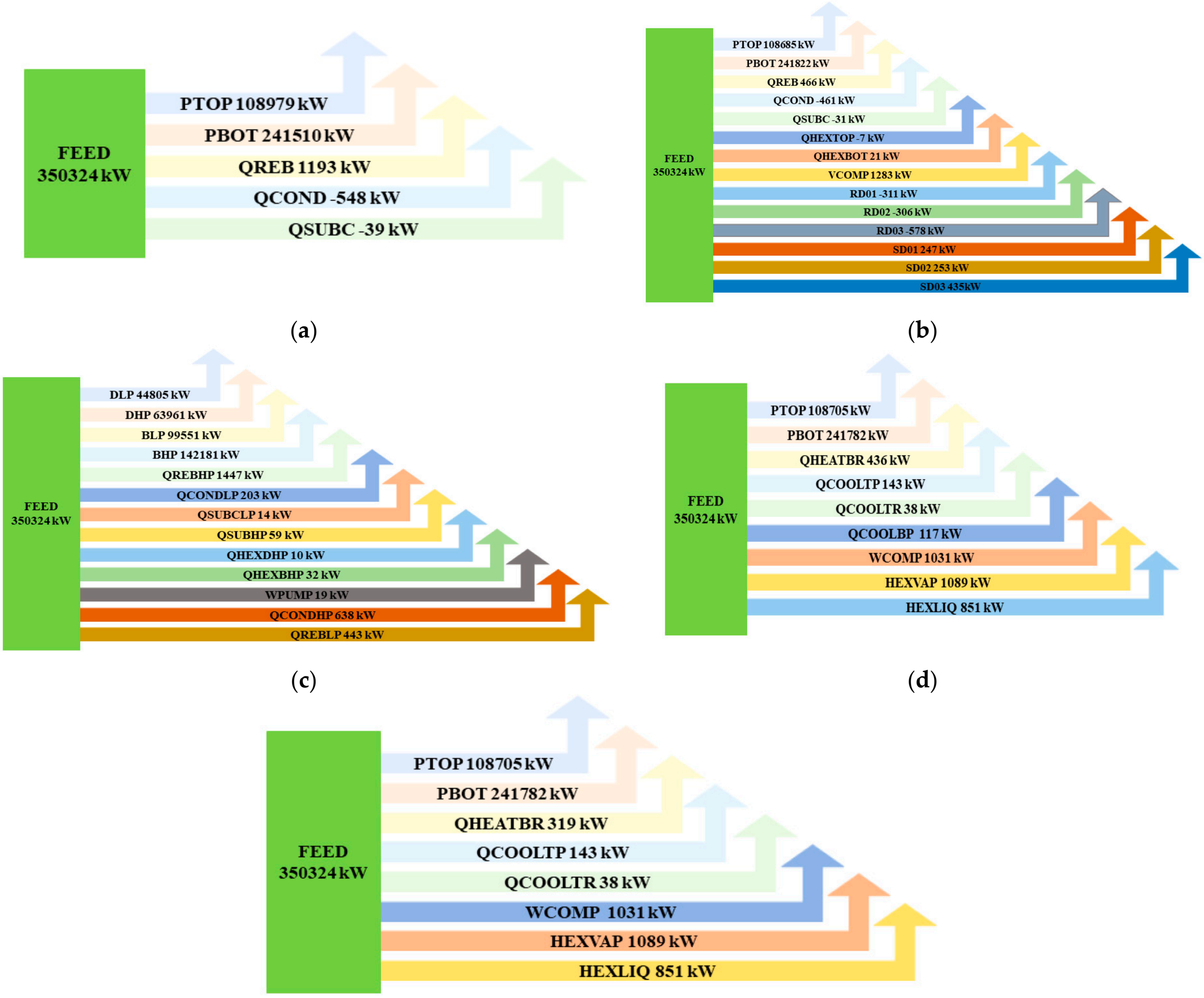

(**a**) (**b**)

(**c**) (**d**)

(**e**)

Figure 6. Exergy flow diagrams of (**a**) CDC, (**b**) iHIDiC, (**c**) EHIDIC, (**d**) VRC, and (**e**) Modified VRC.

Table 8. A comparison of the exergy efficiencies of various heat-integrated designs.

System	Overall Exergy Efficiency	Improvement over CDC (Absolute)	Improvement over CDC (Relative)
CDC	9.27%	—	—
iHIDiC	8.09%	–1.18%	–12.76%
EHIDDiC	9.77%	0.51%	5.47%
VRC (conventional)	9.27%	0.00%	0.02%
VRC (modified)	10.69%	1.42%	15.32%

4. Conclusions

Simulation studies have shown that heat integration in distillation processes is a promising technology with the potential for significant energy and cost savings. However, most studies have directly compared the total utility requirements for alternative designs without the consideration for the quality of the energy involved. Since exergy provides a measure of both the quantity and quality of energy available in a process, exergy efficiency is a more suitable measure for the comparison of alternative designs.

In this study, a conventional industrial-scale i-butane/n-butane fractionator has been selected as a case study for the comparison of the exergy efficiencies of various heat-integrated designs. While all heat integration schemes explored in this project show an apparent reduction in total utility requirements, a proportional increase in overall exergy efficiency is not observed in all cases. These results show that when comparing alternative designs, the type of energy (e.g., thermal or mechanical), as well as the temperature at which a utility is required, must be taken into consideration. Moreover, appropriate matching of hot and cold streams when implementing heat integration in a system is also critical.

Based on overall exergy efficiency, a modified VRC system (η_E = 10.69%) is the most efficient design for this separation, achieving almost 15% higher exergy efficiency relative to the existing CDC system. The exergy efficiency of the conventional VRC system is the same as that of the CDC (η_E = 9.27%). The EHIDDiC system (η_E = 9.77%) is somewhat better than the CDC, whereas iHIDiC shows poor exergy efficiency (η_E = 8.09%), even lower than the CDC.

To further increase the exergy efficiency of the heat pump assisted distillation column, the future research work will be focused on the optimization of the flowrate of the working fluid of the process studied. The optimization of the flow rate will be done either by by-passing the fluid or recycling the working fluid. The exergy analysis will be studied thoroughly by performing the optimization of the fluid flow rate.

Author Contributions: A.J. and A.H. have contributed equally to this work. A.J. and A.H.: Conceptualization, A.J. and A.H.: Writing—Original Draft, A.J., A.H., M.B., U.A., A.R., R.M., T.A., M.M., H.R.L., P.L.S. and K.S.K.: Writing—Review and Editing, A.J. and A.H.: Visualization, M.B., U.A., P.L.S. and K.S.K.: Supervision. All authors have read and agreed to the published version of the manuscript.

Funding: This research received no external funding.

Institutional Review Board Statement: Not applicable.

Informed Consent Statement: Not applicable.

Data Availability Statement: Data is contained within the article.

Acknowledgments: This work was supported by the Chemical Engineering Department, Khwaja Fareed University of Engineering and Information Technology, Rahimyar Khan, Punjab Pakistan.

Conflicts of Interest: The authors declare that they have no known competing financial interest or personal relationships that could have appeared to influence the work reported in this paper.

References

1. de Koeijer, G.; Kjelstrup, S. Minimizing entropy production rate in binary tray distillation. *Int. J. Appl. Thermodyn.* **2000**, *3*, 105–110.
2. Jana, A.K. Heat integrated distillation operation. *Appl. Energy* **2010**, *87*, 1477–1494.
3. Sholl, D.S.; Lively, R.P. Seven chemical separations to change the world. *Nature* **2016**, *532*, 435–437. [CrossRef]
4. Siefert, N.S.; Litster, S. Exergy and economic analyses of advanced IGCC–CCS and IGFC–CCS power plants. *Appl. Energy* **2013**, *107*, 315–328. [CrossRef]
5. Caliskan, H.; Dincer, I.; Hepbasli, A. Energy, exergy and sustainability analyses of hybrid renewable energy based hydrogen and electricity production and storage systems: Modeling and case study. *Appl. Therm. Eng.* **2013**, *61*, 784–798. [CrossRef]
6. Wu, Y.; Yang, W.; Blasiak, W. Energy and exergy analysis of high temperature agent gasification of biomass. *Energies* **2014**, *7*, 2107–2122. [CrossRef]
7. Sorrell, S. Reducing energy demand: A review of issues, challenges and approaches. *Renew. Sustain. Energy Rev.* **2015**, *47*, 74–82. [CrossRef]
8. Saidur, R.; BoroumandJazi, G.; Mekhilef, S.; Mohammed, H.A. A review on exergy analysis of biomass based fuels. *Renew. Sustain. Energy Rev.* **2012**, *16*, 1217–1222. [CrossRef]
9. Kiss, A.A. *Advanced Distillation Technologies: Design, Control and Applications*; John Wiley & Sons, Ltd.: Hoboken, NJ, USA, 2013.

10. Suphanit, B. Design of internally heat-integrated distillation column (HIDiC): Uniform heat transfer area versus uniform heat distribution. *Energy* **2010**, *35*, 1505–1514. [CrossRef]
11. Gadalla, M.; Jiménez, L.; Olujic, Z.; Jansens, P.J. A thermo-hydraulic approch to conceptual design of an internally heat-integrated distillation column (i-HIDiC). *Comput. Chem. Eng.* **2007**, *31*, 1346–1354. [CrossRef]
12. Kiss, A.A.; Olujić, Ž. A review on process intensification in internally heat-integrated distillation columns. *Chem. Eng. Process* **2014**, *86*, 125–144. [CrossRef]
13. Chen, H.; Huang, K.; Wang, S. A novel simplified configuration for an ideal heat-integrated distillation column (ideal HIDiC). *Sep. Purif. Technol.* **2010**, *73*, 230–242. [CrossRef]
14. Seader, J.D. Continuous Distillation Apparatus and Method. U.S. Patent No. 4234391, 18 November 1980.
15. de Graauw, J.; Steenbakker, M.J.; de Rijke, A.; Olujic, Z.; Jansens, P.J. Distillation Column with Heat Integration. The Netherlands Patent Dutch Patent No. P56921NL00, 22 January 2003.
16. Aso, K.; Matsuo, H.; Noda, H.; Takada, T.; Kobayashi, N. Heat Integrated Distillation Column. U.S. Patent No. 5783047, 21 July 1998.
17. Tung, H.-H.; Davis, J.F.; Mah, R.S.H. Fractionating condensation and evaporation in plate–fin devices. *AIChE J.* **1986**, *32*, 1116–1124. [CrossRef]
18. Satoh, T. This Distillation Column Promises Substantial Energy Reductions. Chemical Engineering. Available online: https://www.chemengonline.com/this-distillation-column-promises-substantial-energy-reductions/ (accessed on 13 January 2022).
19. Suphanit, B. Optimal heat distribution in the internally heat-integrated distillation column (HIDiC). *Energy* **2011**, *36*, 4171–4181. [CrossRef]
20. Huang, K.; Liu, W.; Ma, J.; Wang, S. Externally heat-integrated double distillation column (EHIDDiC): Basic concept and general characteristics. *Ind. Eng. Chem. Res.* **2010**, *49*, 1333–1350. [CrossRef]
21. Wang, Y.; Huang, K.; Wang, S. A Simplified Scheme of Externally Heat-Integrated Double Distillation Columns (EHIDDiC) with Three External Heat Exchangers. *Ind. Eng. Chem. Res.* **2010**, *49*, 3349–3364. [CrossRef]
22. Jana, A.K. Advances in heat pump assisted distillation column: A review. *Energy Convers. Manag.* **2014**, *77*, 287–297. [CrossRef]
23. Kazemi, A.; Hosseini, M.; Mehrabani-Zeinabad, A.; Faizi, V. Evaluation of different vapor recompression distillation configurations based on energy requirements and associated costs. *Appl. Therm. Eng.* **2016**, *94*, 305–313. [CrossRef]
24. Shahandeh, H.; Mins, J.; Kasiri, N.; Ivakpour, J. Economic optimization of heat pump-assisted distillation columns in methanol-water separation. *Energy* **2015**, *80*, 496–508. [CrossRef]
25. Annakou, O.; Mizsey, P. Rigorous investigation of heat pump assisted distillation. *Heat Recovery Syst. CHP* **1995**, *15*, 241–247. [CrossRef]
26. Papastathopoulou, H.S.; Luyben, W.L. Control of a binary side stream distillation column. *Ind. Eng. Chem. Res.* **1991**, *30*, 705–713. [CrossRef]
27. Zhu, Z.; Ri, Y.; Jia, H.; Li, X.; Wang, Y.; Wang, Y. Process evaluation on the separation of ethyl acetate and ethanol using extractive distillation with ionic liquid. *Sep. Purif. Technol.* **2017**, *181*, 44–52. [CrossRef]
28. Wang, Y.; Zhang, Z.; Zhao, Y.; Liang, S.; Bu, G. Control of Extractive Distillation and Partially Heat-Integrated Pressure-Swing Distillation for Separating Azeotropic Mixture of Ethanol and Tetrahydrofuran. *Ind. Eng. Chem. Res.* **2015**, *54*, 8533–8545. [CrossRef]
29. Li, M.; Cui, Y.; Shi, X.; Zhang, Z.; Zhao, X.; Zhu, X.; Gao, J. Simulated annealing-based optimal design of energy efficient ternary extractive dividing wall distillation process for separating benzene-isopropanol-water mixtures. *Chin. J. Chem. Eng.* **2020**, *33*, 203–210. [CrossRef]
30. Wang, C.; Guang, C.; Cui, Y.; Wang, C.; Zhang, Z. Compared novel thermally coupled extractive distillation sequences for separating multi-azeotropic mixture of aceton trile/benzene/methanol. *Chem. Eng. Res. Des.* **2018**, *136*, 513–528. [CrossRef]
31. Brito, K.D.; Cordeiro, G.M.; Figueirêdo, M.F.; Vasconcelos, L.G.S.; Brito, R.P. Economic evaluation of energy saving alternatives in extractive distillation process. *Comput. Chem. Eng.* **2016**, *136*, 185–196. [CrossRef]
32. Luo, H.; Bildea, C.S.; Kiss, A.A. Novel heat-pump-assisted extractive distillation for bioethanol purification. *Ind. Eng. Chem. Res.* **2015**, *54*, 2208–2213. [CrossRef]
33. Qi, J.; Tang, J.; Zhang, Q.; Wang, Y.; Chen, H.; Zhao, H.; Zhang, L. Heat-integrated azeotropic distillation and extractive distillation for the separation of heterogeneous ternary azeotropes of diisopropyl ether/isopropyl alcohol/water. *Ind. Eng. Chem. Res.* **2019**, *58*, 20734–20745. [CrossRef]
34. Cui, F.; Cui, C.; Sun, J. Simultaneous optimization of heat-integrated extractive distillation with a recycle feed using pseudo transient continuation models. *Ind. Eng. Chem. Res.* **2018**, *57*, 15423–15436.
35. Cui, P.; Zhao, F.; Yao, D.; Ma, Z.; Li, S.; Li, X.; Wang, L.; Zhu, Z.; Wang, Y.; Ma, Y.; et al. Energy Saving Exploration of Mixed Solvent Extractive Distillation Combined with Thermal Coupling or Heat Pump Technology for the Separation of an Azeotrope Containing Low-Carbon Alcohol. *Ind. Eng. Chem. Res.* **2020**, *59*, 13204–13219. [CrossRef]
36. Jian, X.; Li, J.; Ye, Q.; Yan, L.; Li, X.; Xie, L.; Zhang, J. Intensification and analysis of extractive distillation processes with preconcentration for separating ethyl acetate, isopropanol and water azeotropic mixtures. *Sep. Purif. Technol.* **2022**, *287*, 120499. [CrossRef]
37. Yang, A.; YangKong, Z.; Sunarso, J. Design and optimization of novel hybrid side-stream reactive-extractive distillation for recovery of isopropyl alcohol and ethyl acetate from wastewater. *Chem. Eng. J.* **2022**, *451*, 138563. [CrossRef]

38. Klemola, K.T.; Ilme, J.K. Distillation efficiencies of an industrial-scale i-butane/n-butane fractionator. *Ind. Eng. Chem. Res.* **1996**, *35*, 4579–4586. [CrossRef]
39. Ilme, J.; Klemola, K.; Aittamaa, J.; Nyström, L. Calculating distillation efficiencies of multicomponent i-butane/n-butane column. *Chem. Eng. Commun.* **2001**, *184*, 1–21. [CrossRef]
40. BoroumandJazi, G.; Rismanchi, B.; Saidur, R. A review on exergy analysis of industrial sector. *Renew. Sustain. Energy Rev.* **2013**, *27*, 198–203. [CrossRef]
41. Haragovics, M.; Mizsey, P. A novel application of exergy analysis: Lean manufacturing tool to improve energy efficiency and flexibility of hydrocarbon processing. *Energy* **2014**, *77*, 382–390. [CrossRef]
42. Kencse, H. Complex Evaluation Methodology for Energy-Integrated Distillation Columns. Ph.D. Thesis, Budapest University of Technology and Economics, Budapest, Hungary, 2009.
43. Winterbone, D.E.T. *Ali Advanced Thermodynamics for Engineers*; Butterworth-Heinemann: Oxford, UK, 2015.
44. Kotas, T.J. *The Exergy Method of Thermal Plant Analysis*; Anchor Brendon Ltd.: Tiptree, UK, 1985.
45. Yang, Q.; Qian, Y.; Wang, Y.; Zhou, H.; Yang, S. Development of an Oil Shale Retorting Process Integrated with Chemical Looping for Hydrogen Production. *Ind. Eng. Chem. Res.* **2015**, *54*, 6156–6164. [CrossRef]
46. Sun, J.; Wang, F.; Ma, T.; Gao, H.; Wu, P.; Liu, L. Energy and exergy analysis of a five-column methanol distillation scheme. *Energy* **2012**, *45*, 696–703. [CrossRef]
47. Morris, D.R.; Szargut, J. Standard chemical exergy of some elements and compounds on the planet Earth. *Energy* **1986**, *11*, 733–755. [CrossRef]
48. Ayres, R.U.; Ayres, L.W. *Accounting for Resources, 2: The Life Cycle of Materials*; Edward Elgar Publishing, Inc.: Cheltenham, UK, 1999.
49. Shabbir, K. A Comparison of the Performance of Conventional and Internally Heat-Integrated Distillation Columns. Master's Thesis, University of Engineering & Technology, Lahore, Pakistan, 2016.
50. Javed, S. A Comparison of the Performance of Conventional and Externally Heat-Integrated Double Distillation Columns. Master's Thesis, University of Engineering & Technology, Lahore, Pakistan, 2017.
51. Khan, M.J. A Comparison of the Performance of Various Vapor Recompression Distillation Configurations. Master's Thesis, University of Engineering & Technology, Lahore, Pakistan, 2017.